Oscillatory Turing Patterns in Reaction-Diffusion Systems with Two Coupled Layers

Lingfa Yang and Irving R. Epstein*

Department of Chemistry and Center for Complex Systems, MS 015, Brandeis University, Waltham, Massachusetts 02454-9110, USA
(Received 12 December 2002; published 1 May 2003)

A model reaction-diffusion system with two coupled layers yields oscillatory Turing patterns when oscillation occurs in one layer and the other supports stationary Turing structures. Patterns include "twinkling eyes," where oscillating Turing spots are arranged as a hexagonal lattice, and localized spiral or concentric waves within spotlike or stripelike Turing structures. A new approach to generating the short-wave instability is proposed.

Turing patterns [1–3] typically consist of hexagonal arrays of spots or labyrinthine arrangements of stripes with a single characteristic wavelength. Recently, two-wavelength Turing patterns, referred to as "black-eye" patterns, have been reported in experiments [4,5]. We have shown [6] that spontaneous formation of black-eye patterns in a homogeneous two-dimensional reaction-diffusion system may arise from spatial resonance between two Turing modes and that other resonant patterns, as well as superposition patterns, are also possible. Several of these results have been verified in experiments in which a single Turing mode is subjected to external spatially periodic forcing [7].

Classical Turing patterns are stationary. However, the "twinkling eye" is an oscillatory Turing pattern [6], in which eyelike Turing spots are arranged in a hexagonal lattice, and each spot periodically oscillates 120° out of phase with its nearest neighbor spots. Unlike standing waves, which in reaction-diffusion systems are associated with the short wavelength instability (wave instability), the twinkling-eye pattern is a mixed-mode pattern, which originates from the interaction between a subharmonic Turing mode and an oscillatory mode [6]. In this Letter, we examine the possibility that the interaction of stationary Turing and oscillatory wave modes may lead more generically to a family of oscillating Turing-like patterns.

Several earlier investigations of interacting Hopf and Turing instabilities have been reported [8,9], and we have studied pattern formation resulting from interacting Turing and wave instabilities [10]. A key difference is that in those works the two modes are typically well separated, with the Hopf or wave instability appearing at significantly lower wave number than the Turing mode. Here, the two instabilities may overlap, and the Turing mode can have the lower wave number, resulting in a wealth of new patterns.

Standing waves are well known in electromagnetic and mechanical systems, but standing waves of chemical concentrations are rarely observed. Standing waves in reaction-diffusion systems arise from a wave instability, which requires unequal diffusivities of chemical species. Although standing waves have been seen in binary fluid convection, nematic liquid crystals, and heterogeneous chemical and electrochemical systems [11], it is difficult to satisfy the condidtions for their appearance in homogeneous reaction-diffusion systems like the Belousov-Zhabotinsky (BZ) reaction [10]. This problem may be solved by employing two coupled thin layers. Reactants in each layer have the same diffusivity, but they may be slowed significantly in one layer compared with the other because of physical (e.g., viscosity) or chemical (e.g., complex formation with gel-bound species [12]) reasons. We demonstrate that the wave instability can arise through this layer-coupling mechanism.

In our earlier work [6] we modeled the twinkling-eye pattern with an abstract Brusselator scheme involving cubic autocatalysis. Here we consider a more realistic model: an extended Oregonator with quadratic autocatalysis that mimics the BZ reaction and has been used to study Turing-wave interaction [10] as well as inwardly propagating spirals (antispirals) in a BZ microemulsion [13]. Our model here consists of two linearly coupled extended Oregonators. Reproducing the twinkling-eye pattern indicates that the complexity of pattern formation stems primarily from the coupling and differential diffusivity, rather than from the details of the chemical kinetics.

The experimental arrangement that corresponds to our model is shown in Fig. 1. The layers at the top and the bottom are reaction layers, while the middle layer provides the coupling. We consider two reactive species. One, the "free" species, diffuses through the coupling layer, but the other, "partner," is confined to the reactive layers. The variables x (top), r (middle), and u (bottom) designate the concentration of the free species in the three layers. The partner concentrations are z (top) and w (bottom). Because there is no partner in the middle layer, no reaction occurs there. Such a situation might be realized experimentally with a sandwich of three membranes, in which the middle one is impermeable to one species. We translate our scheme into a five-component reaction-diffusion model:
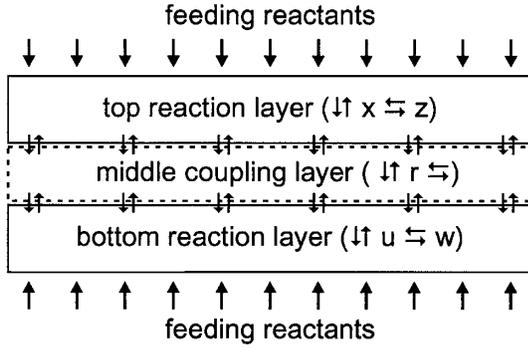
FIG. 1. A system of coupled layers with two-sided feeding, described by models (1)–(5).

$$\frac{\partial x}{\partial t} = D_x \nabla^2 x + F(x, z) - \frac{1}{\delta}[x - r], \tag{1}$$

$$\frac{\partial z}{\partial t} = D_z \nabla^2 z + G(x, z), \tag{2}$$

$$\frac{\partial r}{\partial t} = D_r \nabla^2 r + \frac{1}{\delta}[x - r] + \frac{1}{\overline{\delta}}[u - r], \tag{3}$$

$$\frac{\partial u}{\partial t} = D_u \nabla^2 u + \overline{F}(u, w) - \frac{1}{\overline{\delta}}[u - r], \tag{4}$$

$$\frac{\partial w}{\partial t} = D_w \nabla^2 w + G(u, w), \tag{5}$$

where the diffusion coefficients D_x, D_z, D_r, D_u, and D_w characterize two-dimensional horizontal motion within the layers. The functions F and G describe the reaction kinetics, for which we employ a simple two-variable Oregonator model [14], specified in Eqs. (6) and (7). The terms involving δ and $\overline{\delta}$ give the time scale of the linear coupling between top and bottom layers via local vertical diffusion:

$$F(x, z) = \frac{1}{\epsilon}\left[x - x^2 - fz\frac{x - q}{x + q}\right], \tag{6}$$

$$G(x, z) = x - z. \tag{7}$$

The kinetic parameters ϵ, f, and q are from the Oregonator model [14]. The function $\overline{F}$ is identical to F, except that the kinetic parameters for the top and bottom $(\overline{\epsilon}, \overline{f}, \overline{q})$ layers may differ because the layers are fed with different concentrations of reactants.

The top and bottom layers may show different instabilities when uncoupled because their parameters differ. Physically, the gels may be prepared or fed differently, different membranes may be used, or one may subject the layers to different intensities of illumination. The strength of the coupling, characterized by the δ parameters, may be controlled by adjusting the thickness of the middle layer.

We applied linear stability analysis to the five-component model (1)–(5) to obtain dispersion relations. This analysis indicates that onset of a Turing instability in the bottom layer is determined by the ratio D_u/D_w, and

its location, k_c, is determined by the product, $D_u D_w$. The Turing instability also depends on the chemical feed, which is characterized by the control parameter pair $(\overline{\epsilon}, \overline{f})$. The top layer serves as a wave layer, where waves emerge from a Hopf or wave instability, and the instability is controlled by the feed, i.e., by (ϵ, f).

We performed a series of two-dimensional simulations; in each, the initial condition was always a small amplitude random perturbation of the uniform steady state, and patterns developed spontaneously. When the system reached a stable state (stationary or oscillatory), we took a snapshot with gray levels linearly proportional to the free species concentration and white (black) corresponding to high (low). The physical size of the system was 256×256 space units unless otherwise specified. Periodic boundary conditions were employed in all cases. We fixed parameters $q = \overline{q} = 0.01$ and set coupling parameters $\delta = 2\epsilon$, $\overline{\delta} = 2\overline{\epsilon}$ for simplicity. The feed parameter pairs (ϵ, f) or $(\overline{\epsilon}, \overline{f})$ served as our control parameters.

A typical oscillatory Turing pattern arising from interacting oscillatory and Turing modes is shown in Fig. 2. A Turing structure consisting of hexagonally arranged spots quickly develops [$t = 120$ in Fig. 2(c)], but, instead of maintaining a constant concentration, each Turing spot begins to oscillate [$t = 500$ in Fig. 2(c)]. During the oscillation, the spots adjust their locations to form a hexagonal lattice [Fig. 2(a)], and their phases, randomly distributed initially, gradually synchronize. The synchronized oscillation breaks the original spatial symmetry, D_6, into three subgroups of symmetry D_3 [Fig. 2(b)]. The three subgroups oscillate with the same frequency and amplitude, but with phase difference $2\pi/3$ [Fig. 2(d)], and wavelength $\sqrt{3}$ longer than that of the original lattice. We call such patterns twinkling-eye patterns [6,15].

The evolution of this pattern can be followed at a single point in the center of a spot [Fig. 2(c)]. We clearly see three distinct stages: uniform steady state, stationary Turing pattern, and oscillatory Turing pattern, with the two transitions between the states. We emphasize that this twinkling-eye pattern arises spontaneously from the homogeneous steady state due to the Turing instability. The transition from the stationary to the oscillatory Turing pattern is also spontaneous, indicating that the stationary Turing structure is only metastable. Its instability results from coupling to the oscillatory mode. The dispersion relation [Fig. 2(e)] shows that the most positive mode is a Turing instability, so that the Turing structure grows quickly. The second instability is a wave instability, which generates the oscillation. The symmetry breaking of the D_6 hexagonal lattice arises from the subharmonic Turing mode, which is close to onset.

The twinkling-eye pattern is the only stable solution for this set of parameters. All initial conditions—bulk oscillation, Turing structure, uniform steady state, or random—reach this same final state, which is stable to perturbation and persists indefinitely.
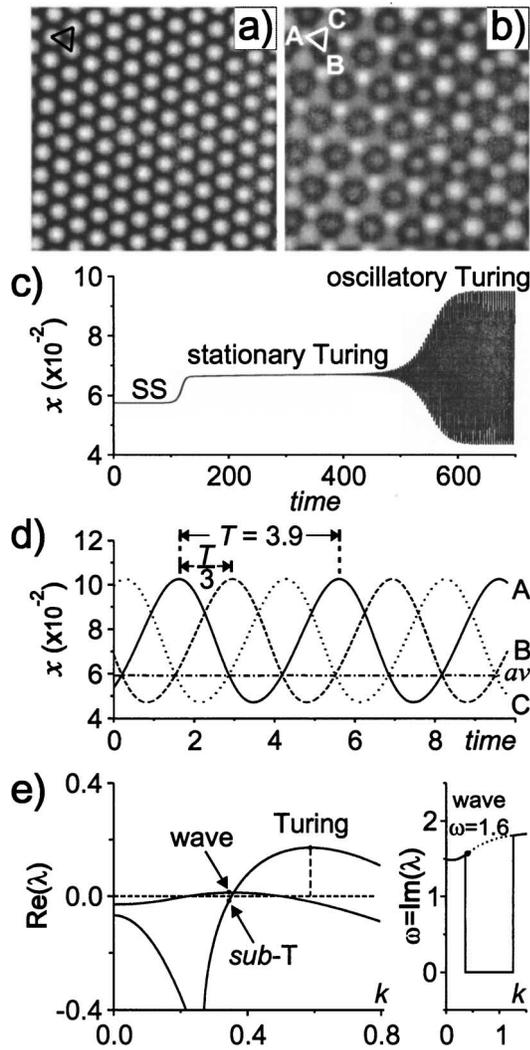
FIG. 2. Formation of a twinkling-eye pattern. Simulation with random initial conditions, parameters $(\epsilon, f) = (0.23, 1.4)$, $(\overline{\epsilon}, \overline{f}) = (0.5, 1.1)$, and diffusion coefficients $(D_x, D_z, D_r, D_u, D_w) = (0.17, 0.17, 6, 0.5, 12)$. Snapshot (a) of u (bottom layer) shows a hexagonal spotlike Turing structure ($\lambda_0 = 12.8$). Snapshot (b) of x (top layer) shows three sets of sublattices ($\lambda = \sqrt{3}\lambda_0$). (c) Concentration changes from uniform steady state (SS) to stationary Turing to oscillatory Turing at a single point. (d) Three-phase oscillations at points A, B, and C of (b). The spatial average of x is nearly constant and close to the steady state value, $x_{SS} = 5.75 \times 10^{-2}$. (e) Dispersion curves of the two most positive eigenvalues. The most positive mode is a Turing instability. The second mode is a short wave instability, which coincides with a subharmonic Turing mode (sub-T). The right-hand plot is the imaginary part corresponding to the most positive eigenvalue. Oscillation period $T = 2\pi/\omega = 3.9$.

As the wavelength of the Turing patterns changes, other types of oscillatory Turing patterns can be found. For long Turing wavelengths, short wavelength traveling waves appear on the Turing structures. Figure 3 shows three examples of this phenomenon [15], where the Turing wavelength is about 4 times longer than that of

the traveling waves. Isolated stable spirals or sustained concentric waves (targets) can be seen on a spotlike Turing structure in Fig. 3(a). Traveling waves, which begin as localized spirals, propagate along labyrinthine Turing stripes in Fig. 3(b). The example in Fig. 3(c) shows short wavelength spiral waves rotating around the oscillatory core to form "pinwheels," where the honeycomb Turing spots arise first, arrange themselves into a hexagonal lattice, then begin to oscillate, and finally develop spirals centered at their cores. The location of the three types of typical Turing structures, spots, stripes, and honeycomb, is shown in a bifurcation diagram in Fig. 3(d).

Stable spirals and sustained concentric waves (targets) are both generated from the wave instability, which determines their common frequency. Since they have the same frequency, they can coexist, unlike the situation in excitable media, where spirals generally have higher frequency, and hence annihilate the lower frequency targets.

To our knowledge, the hexagonally arranged isolated spirals and targets in Fig. 3(a) and the "pinwheel" spirals in Fig. 3(c) have not previously been observed. The pattern in Fig. 3(b) resembles that seen in experiments in which waves in a photosensitive BZ system are guided by a feedback-controlled pattern of illumination [16]. However, our pattern appears spontaneously from the homogeneous uniform state, without any preset pattern or illumination control, with the waves propagating through the labyrinthine "channel" created by the Turing instability.
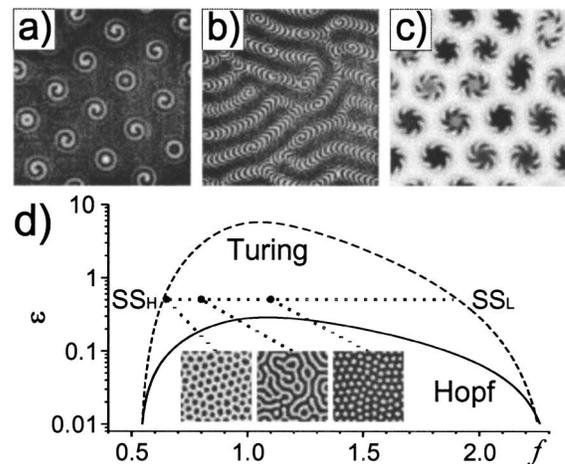

FIG. 3. Waves on Turing structures. Common parameters are $D_x = D_z = D_r = 0.1$, $D_w = 100$. Sizes: (a),(c) 128×128; (b) 256×256. (a) Isolated spirals or targets on hexagonal array of Turing spots. $(\epsilon, f) = (0.14, 16)$, $(\overline{\epsilon}, \overline{f}) = (0.4, 1.1)$, $D_u = 5$. (b) Traveling waves on labyrinthine stripelike Turing structure. $(\epsilon, f) = (0.14, 1.6)$, $(\overline{\epsilon}, \overline{f}) = (0.3, 0.7)$, $D_u = 10$. (c) "Pinwheels" with short spiral waves rotating around oscillatory cores arranged as a honeycomb hexagonal lattice. $(\epsilon, f) = (0.215, 1.1)$, $(\overline{\epsilon}, \overline{f}) = (0.5, 0.65)$, $D_u = 3$. (d) Three typical Turing structures: honeycomb, stripes, and spots are shown in a bifurcation diagram of the isolated (half) system. $(D_u, D_w) = (3, 100)$.
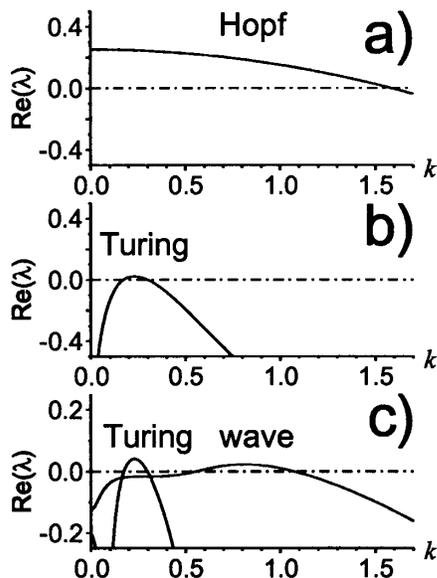
FIG. 4. Short-wave instability resulting from coupling a Hopf oscillation and a stationary Turing solution. (a) and (b) are dispersion relations of the uncoupled systems showing the real part of the most positive eigenvalue. (c) is the dispersion relation of the coupled layer, where an additional wave instability appears. Parameters are as in Fig. 3(c).

The waves in each of the cases in Fig. 3 result from a short-wave instability. Since the short-wave instability generally requires at least three species and at least two levels of diffusivity, one may ask how the instability can arise here with equal diffusion coefficients in the wave layer. Clearly, we cannot have the short-wave instability in the uncoupled homogeneous reaction-diffusion system. With the parameters of Fig. 3(c) and equal diffusion coefficients, the dispersion relations exhibit only a Hopf instability in the uncoupled top layer [Fig. 4(a)], a Turing instability in the uncoupled bottom layer [Fig. 4(b)], and both Turing and wave instabilities in the full system [Fig. 4(c)].

The coupled pattern configuration offers an approach to another challenge, producing standing waves via a short-wave instability in a BZ system. Generating the short-wave instability in homogeneous oscillatory reactions is difficult, because all reactants tend to diffuse at roughly equal rates. In our model system with spatially separated coupled layers, if reactants diffusing in one layer can be slowed significantly compared with the other layer, the coupling can generate a wave instability when the uncoupled layers support oscillatory and stationary (Turing or steady state) modes, respectively. It should be possible to implement such a configuration experimentally by coupling layers of very different viscosity. Alternatively, if the wavelength of the Turing pattern is short compared with that of the wave mode, modulated patterns arise [10].

We have proposed a model that mimics a reaction-diffusion system with two coupled layers to study pattern formation. A novel type of oscillatory Turing pattern is spontaneously formed from interaction between a Turing mode and an oscillatory mode in the two layers. Depending on the wavelength and the structure of the Turing pattern, we find twinkling eyes (Fig. 2), localized spiral or localized concentric waves [Figs. 3(a) and 3(b)], or pinwheels [Fig. 3(c)]. Obtaining oscillatory Turing patterns experimentally may be most easily accomplished in the chlorite-iodide-malonic acid reaction [12]. The proposed configuration should also make it possible to produce wave instability and standing waves by coupling an oscillatory layer with a stationary layer in the classic BZ reaction.

*To whom correspondence should be addressed.
Electronic address: epstein@brandeis.edu
[1] A. M. Turing, Philos. Trans. R. Soc. London B **237**, 37 (1952).
[2] V. Castets, E. Dulos, J. Boissonade, and P. De Kepper, Phys. Rev. Lett. **64**, 2953 (1990).
[3] Q. Ouyang and H. L. Swinney, Nature (London) **352**, 610 (1991).
[4] G. H. Gunaratne, Q. Ouyang, and H. L. Swinney, Phys. Rev. E **50**, 2802 (1994).
[5] C. Zhou, H. Guo, and Q. Ouyang, Phys. Rev. E **65**, 036118 (2002).
[6] L. F. Yang, M. Dolnik, A. M. Zhabotinsky, and I. R. Epstein, Phys. Rev. Lett. **88**, 208303 (2002).
[7] I. Berenstein *et al.* (to be published).
[8] J.-J. Perraud, A. De Wit, E. Dulos, P. De Kepper, G. Dewel, and P. Borckmans, Phys. Rev. Lett. **71**, 1272 (1993); A. DeWit, D. Lima, G. Dewel, and P. Borckmans, Phys. Rev. E **54**, 261 (1996); M. Meixner, A. De Wit, S. Bose, and E. Schöll, Phys. Rev. E **55**, 6690 (1997); S. Bose, P. Rodin, and E. Schöll, Phys. Rev. E **62**, 1778 (2000).
[9] J. Boissonade, E. Dulos, and P. De Kepper, in *Chemical Waves and Patterns*, edited by R. Kapral and K. Showalter (Kluwer, Dordrecht, 1995), p. 221.
[10] L. F. Yang, M. Dolnik, A. M. Zhabotinsky, and I. R. Epstein, J. Chem. Phys. **117**, 7259 (2002).
[11] M. C. Cross and P. C. Hohenberg, Rev. Mod. Phys. **65**, 851 (1993).
[12] I. Lengyel and I. R. Epstein, Science **251**, 650 (1991).
[13] V. K. Vanag and I. R. Epstein, Science **294**, 835 (2001); Phys. Rev. Lett. **87**, 228301 (2001).
[14] R. J. Field and R. M. Noyes, J. Chem. Phys. **60**, 1877 (1974); J. P. Keener and J. J. Tyson, Physica (Amsterdam) **21D**, 307 (1986).
[15] Downloadable movies of these dynamic patterns are available at http://hopf.chem.Brandeis.edu/yanglingfa/pattern/oscTu/index.html.
[16] T. Sakurai, E. Mihaliuk, F. Chirila, and K. Showalter, Science **296**, 2009 (2002).